Int J Thermophys (2008) 29:1719–1729
DOI 10.1007/s10765-008-0443-8

The Limits of a Rayleigh-Scattering Primary Thermometer

M. de Podesta · G. Edwards

Published online: 17 June 2008
© Crown copyright. Reproduced by permission of the Controller of HMSO
and the Queen's printer for Scotland 2008

Abstract Progress in the development of an apparatus to compare the thermodynamic temperature of a gas with the temperature as determined by the International Temperature Scale of 1990 (ITS-90) is reported. The apparatus uses the Rayleigh scattering of light from a gas to provide an intensive measure of gas density, thus avoiding the need for corrections for dead volumes or wall adsorption required by conventional gas thermometry. A laser beam is shone through gas in two cells that are at the same pressure but different temperatures, and the measured ratio of the Rayleigh scattering signals from the two cells can be related to the ratio of the gas density in the cells. From the density ratio, the thermodynamic temperature of one cell can be inferred if the other cell is held close to the triple point of water. However, the Rayleigh scattering is weak and signals are small, making measurements with sufficiently small uncertainty extremely challenging. Since previous reports, the apparatus has been significantly modified, and these changes are described along with indicative results. In this paper, results of measurements in the range from 211 K to 292 K using both argon and xenon are reported. The results suffer from large systematic errors due to contamination in one of the measurement cells. Although the results do not provide reliable estimates of $T - T_{90}$, they indicate that measurements with uncertainties below 1 mK are feasible.

Keywords Gas thermometry · Primary thermometry · Rayleigh scattering

M. de Podesta (✉) · G. Edwards
National Physical Laboratory, Hampton, Teddington, Middlesex TW11 0LW, UK
e-mail: michael.depodesta@npl.co.uk

1 Introduction

1.1 Motivation

Over the last decade, the differences between the thermodynamic temperature, T, and the temperature according to the ITS-90, T_{90}, in the range from −200 °C to 0 °C have become ever more clearly defined [1–5]. This is due to the unprecedentedly small uncertainties offered by acoustic thermometry using quasi-spherical resonators. In addition to the low uncertainties, the acoustic thermometry technique is robust, in that different resonances offer internal consistency checks that reduce its susceptibility to a wide range of possible sources of systematic error. In addition to *internal* consistency, results from around the world using spheres made with a wide range of construction techniques show an impressive degree of inter-laboratory consistency. This agreement is to be welcomed, but raises the question as to whether a single technique of thermometry can be used to define the direction of future corrections to the temperature scale. If we are confident of the physics, then a single technique is perfectly acceptable, but temperature as a concept should apply to all physical systems in equilibrium and it would add to the robustness of the acoustic findings if, *even at a single temperature*, we could confirm the acoustic data with a similar uncertainty level using an alternative technique.

The idea that there might be an undiscovered systematic error in a technique is not at all unfeasible. For example, in the establishment of ITS-90 in this temperature range (which included no data from acoustic thermometry), data from constant-volume gas thermometry (CVGT) [6,7] were used, along with data from a cryogenic radiometer (CR) [8,9]. These differing methods disagreed with each other by more than their combined uncertainties, so clearly there was a problem with one or both of the methods. Furthermore, both methods showed significant differences from more recent acoustic thermometry. The work described here is an attempt to develop an alternative method of gas thermometry that could be used to check the results of acoustic thermometry.

2 The Technique

2.1 Introduction

This apparatus (Fig. 1) has been described elsewhere [10], so here we summarize that previous description and highlight recent developments. An intense beam of green laser light (5 W at $\lambda = 532$ nm) is shone through gas in two cells, A and B, that are at the same pressure P, but different temperatures T_A and T_B. Gas (argon or xenon) purified by slow passage through a getter (SAES GC50) and a 3 nm particulate filter is drawn slowly first through Cell A and then through Cell B by an oil-free pumping system. Mass-flow controllers on the inlet and outlet permit independent control of pressure and flow rate. The cells and associated gas handling system have a total volume of approximately 2 L and typical flow rates through the system are near 5 sccm (3.7 μmol · s^{-1}), resulting in a typical residence time in the apparatus of about 7 h. The apparatus had been flushed with clean argon gas for many months before

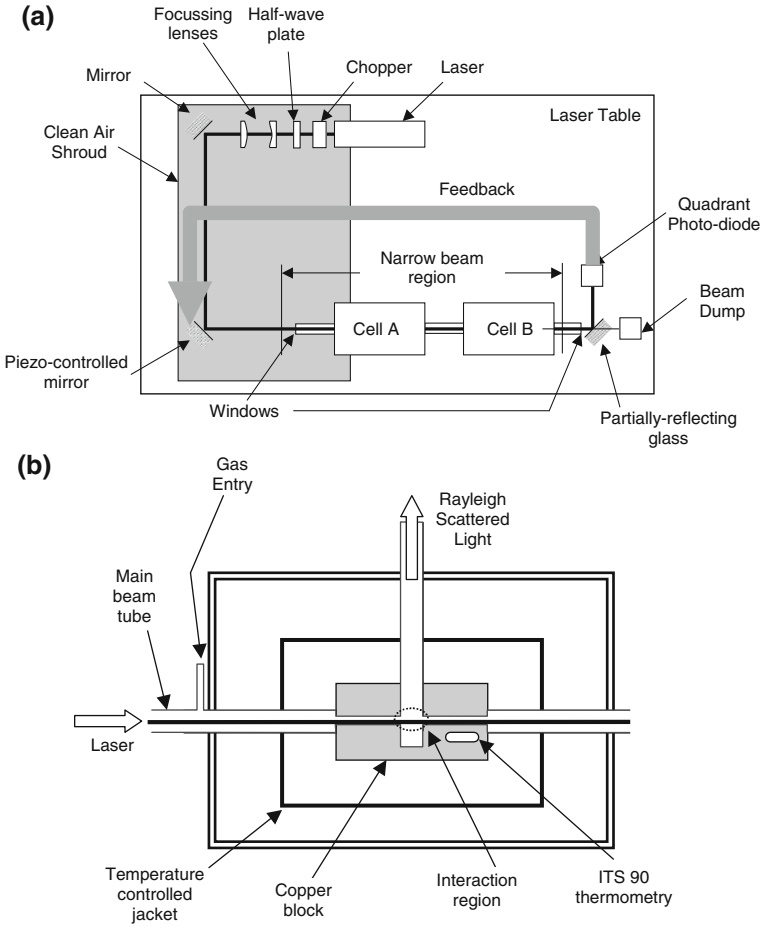

Fig. 1 (**a**) General layout of the apparatus and (**b**) details of an experimental cell

the experiments described below took place, so in principle the apparatus should have been extremely clean. However, as will become clear when we look at the data, despite the care taken, there is strong evidence of contamination in Cell B.

Rayleigh scattering [11] arises from the interaction of molecules with light and, crucially, is an elastic process with no heating of the gas. Since the scattering is weak, the beam intensity is only reduced by a few parts per million in its traversal of the cells. However, detection of the weak scattering presents a significant technical challenge. We observe light scattered from molecules in a 3 mm length of the beam at the center of each cell. The Rayleigh-scattered light is captured by a compact, telecentric optical system, and the light intensity is measured using trap detectors, consisting of 3 Hamamatsu 1331 10 mm × 10 mm photodetectors. The photocurrent is amplified by a transimpedance amplifier utilizing an OPA128LM integrated circuit with a gain of $10^9\ \mathrm{V} \cdot \mathrm{A}^{-1}$. The detector–amplifier combination is thermally insulated

and temperature stabilized to within ±25 mK at about 30 °C. Temperature stabilization minimizes gain changes in the amplifier and the very significant effect of offset drifts, which were much larger than expected and measured to be approximately 5 mV · °C^{-1}. Subsequent investigations have shown that most of this arises from the temperature dependence of the dark current of the large-area photodiodes. In fact, the temperature-induced offset drift is the largest source of electrical 'noise' in the experiment. The electrical signal S_{Rayleigh} from each photodetector is related to the brightness of the scattered light in each cell, which is in turn related to the density of the gas (ignoring virial coefficients) by

$$\begin{aligned} S^{\text{A}}_{\text{Rayleigh}} &\propto \textit{Cell A gas density} = K_{\text{A}} \frac{P}{T_{\text{A}}} \\ S^{\text{B}}_{\text{Rayleigh}} &\propto \textit{Cell B gas density} = K_{\text{B}} \frac{P}{T_{\text{B}}} \end{aligned} \tag{1}$$

where K_{A} and K_{B} are constants for the apparatus. The key advantages of this technique are the highly linear dependence of scattering intensity on density, and the fact that scattering provides an *intensive* measure of gas density. Thus, there is no correction for gas adsorbed in walls, or in 'dead' volumes.

2.2 Experimental Challenges

Three challenges have formed the focus of recent experimental work: (1) minimization of 'spurious' scattering signals, where light is able to reach the detectors without being scattered from the gas; (2) attainment of a sufficient signal-to-noise ratio in the measurement of the weak Rayleigh signals; and (3) maintenance of mechanical and optical stability throughout measurement runs extending for many days. For argon at 290 K and a pressure of 100 kPa, the expected signal level in each cell is 0.1 nW, and to achieve 1 mK of resolution, we need to resolve the 0.1 nW of signal to roughly three parts in 10^6, i.e., to within 0.3 fW. With the apparatus as described below, this results in a signal of approximately 60 mV which must be resolved to within 0.2 μV. For xenon, the signal is roughly 6.35 times larger.

2.2.1 Spurious Scattering

Despite the use of the highest quality optical components, typically 1 % of the light is scattered from the beam by each of the 10 optical surfaces the light meets on its way to the first cell. This light is primarily forward-scattered into a diverging cone of incoherent radiation around the main beam. The effect of this scattering is minimized by the appropriate use of apertures but, by the time the beam enters Cell A, conservatively 10 mW of light is present in this diverging cone. We believe we have eliminated all single-reflection paths into the detector, but double incoherent reflections cannot be avoided and are mitigated by painting surfaces with *Nextel* black paint. In a previous paper [10], we had been able to achieve spurious scattering signals (measured with the cells evacuated) of around 1 pW; this level has now been reduced to 0.1 pW, and

the background shows no discernable drifts over periods of many days. Background scatter at this level represents only one part in 10^{11} of the incoherent scattered light that enters the cells, but we believe that an improved design (mainly widening the beam tube) could reduce this by another factor of 10 or more. This scattering level represents approximately one part in 10^3 of the expected atmospheric-pressure signal from argon. However, it is important to realize that we have no way of distinguishing *changes* in the background signal from *changes* in the Rayleigh signal, and so we need to be confident that the background signal will be constant at this level to better than three parts in 10^3 (i.e., three parts in 10^6 of the overall signal level). The use of apertures is not the ideal way to eliminate spurious scattering because if an aperture is effective in eliminating significant amounts of light then, inevitably, changes in beam position will cause a redistribution of significant amounts of scattered light.

Although the background signal from each cell needs to be constant while the pressure is changed, we do not need to know its value. Experimentally, the signals in the two cells take the form

$$\begin{aligned} S^{\mathrm{A}}_{\mathrm{Rayleigh}} &= K_{\mathrm{A}} \frac{P}{T_{\mathrm{A}}} + \mathit{offset}_{\mathrm{A}} \\ S^{\mathrm{B}}_{\mathrm{Rayleigh}} &= K_{\mathrm{B}} \frac{P}{T_{\mathrm{B}}} + \mathit{offset}_{\mathrm{B}} \end{aligned} \tag{2}$$

where the offset terms arise from spurious scattering. We examine the *correlation* between the Rayleigh signals in the two cells by plotting $S^{\mathrm{B}}_{\mathrm{Rayleigh}}$ versus $S^{\mathrm{A}}_{\mathrm{Rayleigh}}$

$$S^{\mathrm{B}}_{\mathrm{Rayleigh}} = \left[\frac{K_{\mathrm{B}}}{K_{\mathrm{A}}}\frac{T_{\mathrm{A}}}{T_{\mathrm{B}}}\right] S^{\mathrm{A}}_{\mathrm{Rayleigh}} - \left[\frac{K_{\mathrm{B}}}{K_{\mathrm{A}}}\frac{T_{\mathrm{A}}}{T_{\mathrm{B}}}\mathit{offset}_{\mathrm{A}} - \mathit{offset}_{\mathrm{B}}\right] \tag{3}$$

when T_{A} and T_{B} are nearly equal and close to the triple point of water, we can determine the experimental sensitivity $K_{\mathrm{B}}/K_{\mathrm{A}}$. If we subsequently change T_{B} while keeping T_{A} constant, then (to the extent that the experimental sensitivity does not change) we can determine the thermodynamic temperature of Cell B.

2.2.2 Signal Recovery

Previously, the laser beam was chopped at 87 Hz, and the brightness in each cell measured using lock-in detection. However, to optimize noise performance, the transimpedance amplifier gain was increased from 10^7 to 10^9, and the reduction in amplifier bandwidth (to roughly 10 Hz) required a reduction of the chopping frequency. Choppers operating below 10 Hz suffer from significant phase noise (jitter) and so, initially, we opted to reduce the measurement frequency to quasi-DC (less than 0.1 Hz) and use a simple shutter to correct for offset drift. However, this had the consequence that every 10 s or so the cell windows alternately warmed and then cooled. These small changes caused local 'lensing' at the windows, resulting in irreproducibility in the beam position. For this reason, the beam is now left unchopped and passes uninterrupted through both cells at all times; the 'chopping' is performed in the signal detection path. The transimpedance amplifier output from each cell is fed to one of

two Agilent nanovoltmeters, and readings from the two cells are triggered simultaneously. While the nanovoltmeters autonomously collect data from the cells, other experimental data are captured so that over a measurement cycle lasting roughly one minute, there is less than 10 s 'deadtime' when no Rayleigh data are being collected.

3 Indicative Results

3.1 Measurement Procedure

To measure temperatures using this apparatus, we adopted the following procedure. Firstly, the temperature of Cell A was stabilized for the duration of the experiment. The temperature of Cell B was then stabilized at selected values in the range from 211 K to 292 K. The temperature of the copper blocks in the center of the cells is not actively controlled. Instead, the blocks are weakly linked (with a time constant of approximately one day) to a temperature-controlled jacket through which fluid cooled close to the target temperature circulates. The ITS-90 temperature of the two blocks is recorded using capsule-type platinum resistance thermometers placed within the two blocks and is stable to within $20\,\mathrm{mK}\cdot\mathrm{day}^{-1}$.

The pressure during a measurement run is varied using mass-flow controllers at the inlet and outlet, with feedback derived from a high-precision barometer (Druck Model 152). We adopted different pressure-time profiles for argon and xenon. For xenon, which is rather expensive, we set a very low exhaust rate of only 0.1 sccm, and then set the inlet flow to roughly 1 sccm. The pressure rose from <0.1 kPa almost linearly with time. For argon, the exhaust flow was set at 5 sccm and the pressure was swept up and down between 20 kPa and 40 kPa at a rate of typically $5\,\mathrm{kPa}\cdot\mathrm{h}^{-1}$ with the exhaust flow set to a nominal value of typically 5 sccm. Approximately once per minute, the inlet gas flow is adjusted and in this way the pressure can be swept while maintaining a specified flow through the apparatus. The signal profiles from these two experiments are shown in Fig. 2.

The data from Fig. 2 are shown re-plotted in Fig. 3 in the form described by Eq. 3. Before re-plotting, the data from each cell is adjusted to account for background drift between successive light-intensity measurements. These drifts are largely caused by changes in the temperature of the photodiodes, and this compensation is not completely effective. The data are then linearly adjusted to the mean ITS-90 temperature as measured by the capsule PRTs within each cell. Figure 4 shows Rayleigh plots equivalent to Fig. 3 with Cell B at temperatures from 211 K to 292 K, while Cell A was maintained close to 271 K. By comparing the slopes in this figure with the slopes when temperatures in the two cells were both close to the triple point of water, the thermodynamic temperature of Cell B can be determined.

The data in Fig. 4 appear *qualitatively* correct but detailed analysis shows that there is a serious systematic error that unfortunately was not discovered until after all the data had been taken. Figure 5 shows Rayleigh plots for argon and xenon taken with identical flow profiles at the same temperature at the end of the experimental runs. The slopes of these graphs should be equal to better than one part in 10^4, but in fact they differ by around 5 %. The xenon signal in Cell B is lower than expected and this

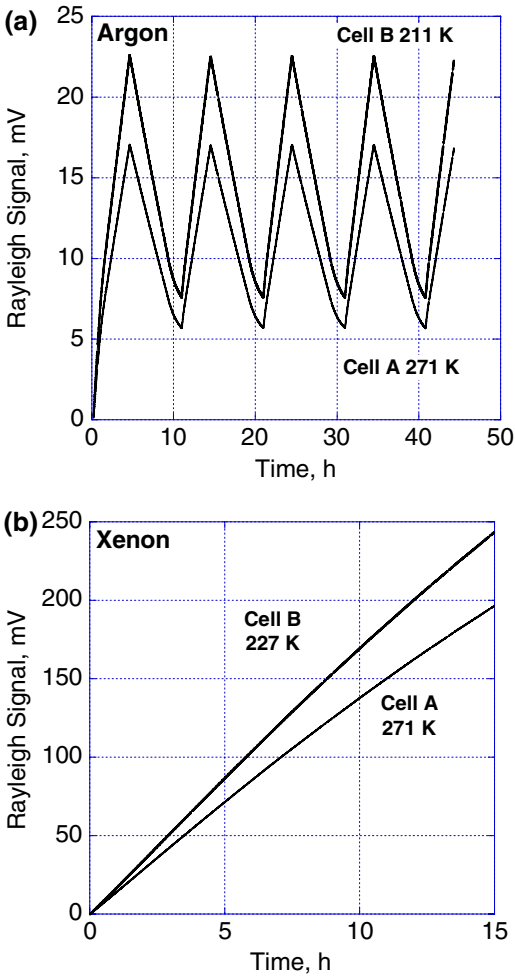

Fig. 2 Rayleigh signals from Cells A and B plotted as a function of time: (**a**) with argon flowing through the cells, the pressure is varied between 100 hPa and 300 hPa and (**b**) with xenon flowing through the cells, the pressure is increased to approximately 550 hPa

is confidently believed to be due to contamination, most probably with water vapor. The Rayleigh signal from a gas is proportional to the square of the difference of the refractive index from unity. Water vapor and air have refractive indices close to that of argon and so contamination did not obviously affect the signal. The higher refractive index of xenon makes the admixture of even a small amount of lower refractive index gas quite noticeable.

3.2 Limiting Uncertainty

While the contamination in Cell B prevented us from meaningfully evaluating $T - T_{90}$, we can estimate the limiting uncertainty on the slope, and thus the limiting uncertainty for future measurements of T using this technique. Figure 6 shows the residuals from a quadratic fit to the data in Fig. 5 and indicates that the signals have a noise component

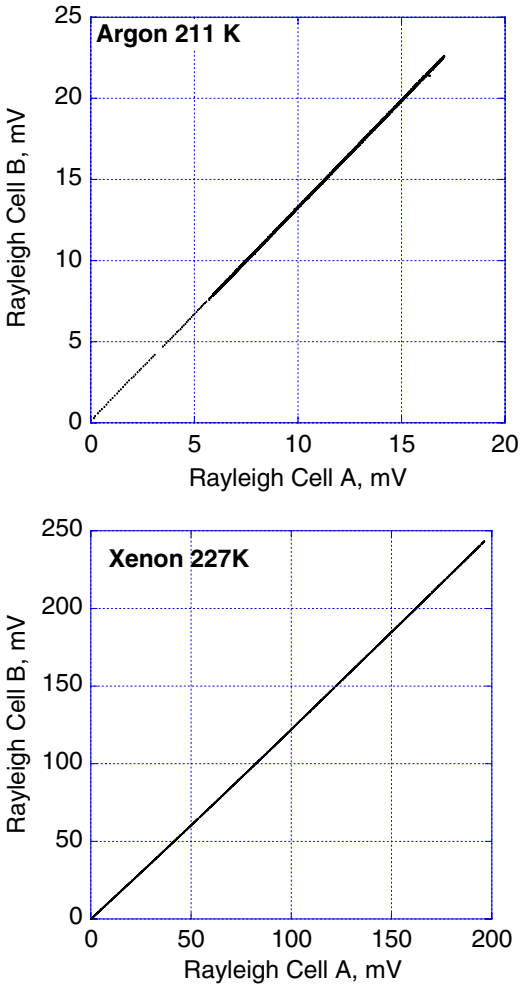

Fig. 3 Data from Fig. 1 re-plotted as Rayleigh plot of the signal in Cell B versus the signal in Cell A

with a standard deviation of around 16 μV, significantly larger than the expected noise level (due to shot noise, Johnson noise, and the NEP of the photodiode) of 5 μV. The excess noise almost certainly arises from the temperature variations of the photodiodes. The minute-to-minute variation of the photodiode temperatures had a standard deviation of 0.003 mK that factors in with the measured offset sensitivity ($5\,\mathrm{mV}\cdot{}^{\circ}\mathrm{C}^{-1}$) to yield roughly 15 μV of minute-to-minute variation in signal. Some attempt was made to correct for this by estimating the background signal for each Rayleigh measurement as the average of the previous and following dark-signal measurements. However, the spectrum of variations means this correction is unlikely to have been completely effective.

However, even using the currently achieved noise level in a model for a pressure sweep from 0 kPa to 50 kPa, the limiting Type A uncertainty in slope for xenon is one part in 10^5, corresponding to 2.5 mK ($k = 1$) uncertainty in temperature. If the

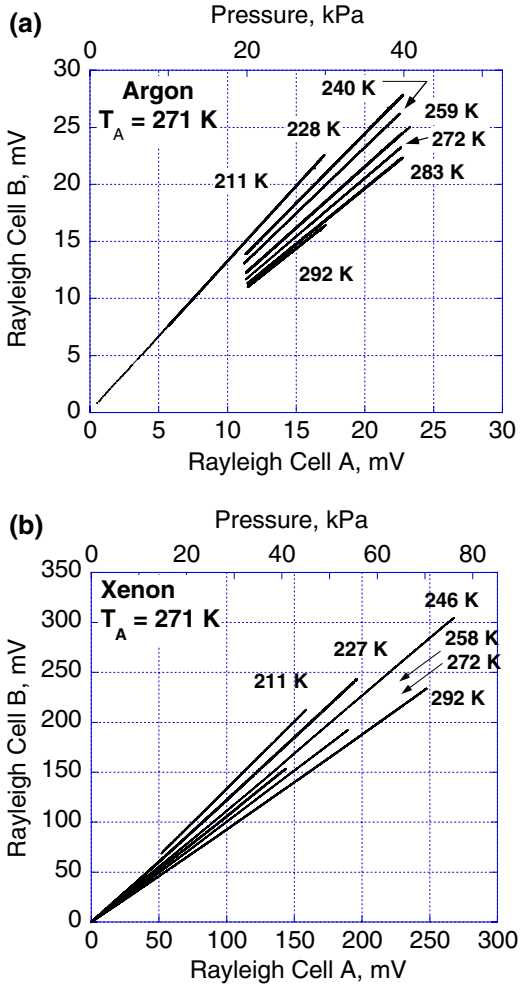

Fig. 4 Rayleigh plots for cell B temperatures in the range of 211 K to 292 K for (**a**) argon and (**b**) xenon

temperature stability of the transimpedance amplifiers was improved, we would expect this uncertainty to be reduced to less than 1 mK. The results scale as the square root of the signal-to-noise ratio, so (for argon) the uncertainty would be increased by a factor ≈ 2.5.

The contamination of Cell B has prevented us from fully assessing the Type B uncertainty contributions, but the largest components are likely to arise from changes in optical gain or spurious scatter signal as either the pressure or temperature changes. By scanning the beam position within the cells using the piezo-controlled mirror, it was possible to show that the beam position did not wander by more than approximately 10 μm vertically or horizontally over periods of months. However, to gain confidence that the optical gain was unchanged (i.e., that the mechanical stability of the optics matched the stability of the beam), it would be necessary to perform many re-alignments of the optical system before, during, and after a measurement run. This process was

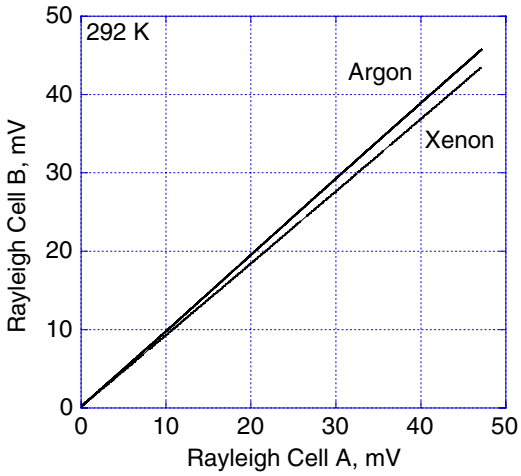

Fig. 5 Rayleigh plot for Cell B at 292 K for argon and xenon. Slopes should be equal if the gas composition is the same in both cells

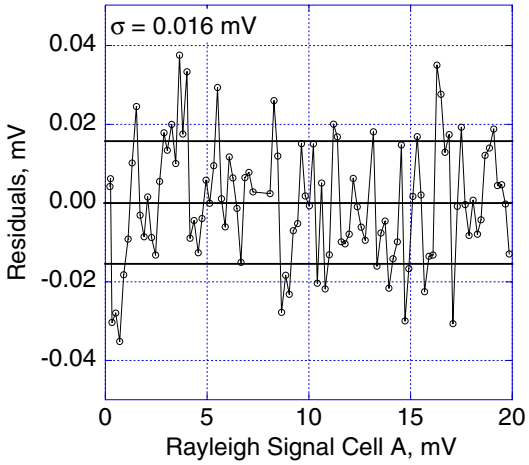

Fig. 6 Residuals from a quadratic fit to a portion of the xenon data from Fig. 5

not automated in this inception of the experiment, but could be in principle, and would provide high confidence in the results.

Virial effects additionally complicate the inference of temperature at the millikelvin level, but closed-form expressions for the intercept, slope, and quadratic curvature of the Rayleigh plots can be obtained. If we consider the Rayleigh plots to have the form

$$S_{\mathrm{B}} = a + bS_{\mathrm{A}} + cS_{\mathrm{A}}^2 \tag{4}$$

then the coefficients can be shown to have the following form:

$$a = offset_{\mathrm{B}} - offset_{\mathrm{A}} \frac{K_{\mathrm{B}} T_{\mathrm{A}}}{K_{\mathrm{A}} T_{\mathrm{B}}} \tag{5}$$

$$b = \frac{K_B T_A}{K_A T_B} - 2 \times offset_A \frac{K_B T_A}{K_A T_B} \left[\frac{T_A}{T_B} \frac{\beta(T_B)}{K_A} - \frac{\beta(T_A)}{K_A} \right] \tag{6}$$

$$c = \frac{K_B T_A}{K_A T_B} \left[\frac{T_A}{T_B} \frac{\beta(T_B)}{K_A} + \frac{\beta(T_A)}{K_A} \right] - 3 \times offset_A \frac{K_B T_A}{K_A T_B} \times \frac{T_A}{T_B} \times \frac{\beta(T_A)}{K_A} \times \frac{\beta(T_B)}{K_A} \tag{7}$$

where $\beta(T)$is the second pressure virial coefficient.

4 Conclusion

We have reported measurements in the range from 211 K to 292 K on a Rayleigh-scattering primary thermometer. Although the apparatus performed as expected, we could not determine results for $T - T_{90}$ because of contamination in one of the cells. An outline assessment of the uncertainties indicates that Type A uncertainties of less than 1 mK ($k = 1$) are achievable and that none of the identified Type B contributions represent fundamental limits to the applicability of the technique. Importantly, the non-contact nature of the technique allows measurements to be made across a wide range of temperatures and the technique could prove of particular significance beyond the current upper limit of acoustic thermometry (≈300 °C).

Acknowledgments This work was supported by the UK Department for Trade and Industry. The author would like to thank Stephanie Bell and Ken Hill for their kindness.

Nomenclature

sccm standard cubic centimeters per minute

References

1. M.B. Ewing, J.P.M. Trusler, J. Chem. Thermodyn. **32**, 1229 (2000)
2. G.F. Strouse, D.R. Defibaugh, M.R. Moldover, D.C. Ripple, in *Temperature: Its Measurement and Control in Science and Industry*, vol. 7, ed. by D.C. Ripple (AIP, Melville, New York, 2003), pp. 31–36
3. G. Benedetto, R.M. Gavioso, R. Spagnolo, P. Marcarino, A. Merlone, Metrologia **41**, 74 (2004)
4. M.R. Moldover, S.J. Boyes, C.W. Meyer, A.R.H. Goodwin, J. Res. Natl. Inst. Stand. Technol. **104**, 11 (1999)
5. L. Pitre, M.R. Moldover, W.L. Tew, Metrologia **43**, 142 (2006)
6. D.N. Astrov, L.B. Beliansky, Y.A. Dedikov, S.P. Polunin, A.A. Zakharov, Metrologia **26**, 151 (1989)
7. R.E. Edsinger, J.F. Schooley J. Res. Natl. Inst. Stand. Technol. **95**, 255 (1990)
8. T.J. Quinn, J.E. Martin, Phil. Trans. Roy. Soc. (London) **316**, 85 (1985)
9. J.E. Martin, T.J. Quinn, B. Chu, Metrologia **25**, 107 (1988)
10. M. de Podesta, G. Edwards, in *Proceedings of TEMPMEKO 2004, 9th International Symposium on Temperature and Thermal Measurements in Industry and Science*, ed. by D. Zvizdić, L.G. Bermanec, T. Veliki, T. Stašić (FSB/LPM, Zagreb, Croatia, 2004), pp. 85–90
11. J.O. Hirchfelder, C.F. Curtis, R.B. Bird, *Molecular Theory of Gases and Liquids* (Chapman and Hall, London, 1954)